Composites of Anionic (Co)polyamides (Nylon 6/Nylon 12) with Short Glass E-Fibers. Preparation and Properties

I. ARVANITOYANNIS[1,*] and E. PSOMIADOU[2]

[1]University of Nottingham, Sutton Bonington Campus, Department of Food Science and Applied Biochemistry, Sutton Bonington, Leics. LE125RD, Loughborough, United Kingdom; [2]Loughborough University of Technology, Department of Chemical Engineering, Loughborough, LE 11 3TU Leics., United Kingdom

SYNOPSIS

The recent high demand of thermoplastic composites has induced an extensive experimentation and utilization of polyamides as thermoplastic sheet composites. The hand layup technique was used for the preparation of the glass fiber polyamide composites studied here. The percentage crystallinity of the composites was determined with a variety of techniques such as differential thermal analysis (DTA), wide-angle X-ray diffraction (WAXD) patterns, and density measurements. Glass transitions (T_g) and melting temperatures (T_m) were determined with DTA and dynamic mechanical thermal analyzer (DMTA) measurements. Finally, the mechanical properties (stress–strain curves and compression tests) were investigated and the results were correlated to the glass fiber content, the void content, and the percentage of the comonomer unit (caprolactam and laurolactam) in the polyamide composite. © 1994 John Wiley & Sons, Inc.

INTRODUCTION

The currently predominant matrix resins for composites continue to be the thermosetting polymers due to their low viscosity (especially in the liquid state) and their facile impregnation into the fiber bundle before the occurrence of curing.[1,2] However, a number of arising disadvantages connected to the production of thermosetting composite resins such as the limited shelf life of the polymers, variation of composite properties, long curing times, limited recyclability, and inadequate impact properties have recently oriented more research work toward the utilization of the thermoplastic composites.[2,3]

The following methods have been used for the production of thermoplastic long- and short-fiber composites: extrusion,[4] solvent impregnation,[2] hand layup,[5] film stacking,[5] melt impregnation,[6] fluidized impregnation of expanded fiber bundles,[2] deposition of a polymer powder/fiber mixture from a water-based slurry,[2,7-9] autoclave bag molding,[1] filament winding,[10,11] pultrusion,[1,12-14] injection molding,[1,4,15] and stamping.[16]

The present article investigates the effect of introducing short glass fibers in a series of (co)polyamides (nylon 6/nylon 12). Previous studies in the field of glass/carbon fiber thermoplastic polyamide composites were focused mainly on homopolyamides such as nylon 6,[17,18] nylon 11,[19] nylon 12,[16,19] nylon 6.10,[19,20] and blends of the latter with polycarbonate,[21,22] which are the most common engineering plastics.

The applicability of this study lies in the growing interest in the use of thermoplastic matrices such as polyphenylene sulfide (PPS)[23] and polyamides[24] or, generally, semicrystalline thermoplastic polymers[20] for the preparation of composite materials. The advantages of using the semicrystalline, thermoplastic (co)polyamides over the thermosets as matrices consist of

a. the possibility of controlling their percentage crystallinity in order to "tailor" the physical or the chemical properties of the (co)polymers instead of the degree of curing (thermosets)[23];

* To whom correspondence should be addressed at Osaka National Research Institute, AIST, Functional Polymer Section, 1-8-31 Midorigaoka, Ikeda, 563 Osaka, Japan.

Journal of Applied Polymer Science, Vol. 51, 1883–1899 (1994)
 CCC 0021-8995/94/111883-17

b. their inherent ease of processing[16];
c. the enhanced composite toughness[16];
d. the more easily repairability than that of the thermosets, and
e. the possibility of their eventual recycling, which is very crucial due to the currently extensive pollution of the environment with nonbiodegradable and/or nonrecyclable polymers.[16,19]

EXPERIMENTAL

Materials

The homopolyamides (nylon 6 and nylon 12) and the (co)polyamides CL/LL (mol/mol 75/25, 50/50, and 25/75) (where CL and LL are caprolactam and laurolactam, respectively) were provided in powder form by CIBA-GEIGY S.A. The short glass E-fibers were also supplied by CIBA-GEIGY S.A.

Preparation of the (Co)polyamide Composites—Hand Layup Method

The mold used for the fabrication of the composite sheet consisted of one middle frame, in which two plates were fitted at the top and bottom, respectively.[20] The molding setup for glass-fiber reinforced (co)polyamide rods was reported previously.[20] E-glass fiber-reinforced (co)polyamide nylon 6/nylon 12 composite (cross-ply) sheets were molded by the hand layup technique.[20] The molding box was kept inside an electric furnace chamber under a load of 2.5 kg on the upper part of the mold at a temperature T_m of +20°C for 30 min. The excess (co)polyamide nylon 6/nylon 12 was squeezed out from the mold. The molding box was removed from the furnace and cooled down according to the following techniques[4]:

(a) quenched in ice water;
(b) cooled in the air at room temperature; and
(c) cooled gradually in the oven.

The thickness of the fabricated glass fiber-reinforced (co)polyamides were 1.5 mm (2 ply), 3 mm (4 ply), 3.5 mm (6 ply), 4 mm (8 ply), and 5 mm (10 ply) with fiber volume fractions of 0.15, 0.225, 0.3, 0.375, and 0.45, respectively.

Characterization of the Neat (Co)polyamides and of the (Co)polyamide Composites

Density Measurements

Densities were determined at 23°C, pycnometrically,[25] with toluene and using a CCl_4/EtOH density gradient column (Davenport) using polymer samples previously degassed at 0.1 mmHg for 2 h.[26]

Differential Thermal Analysis (DTA) Measurements

The glass transitions (T_g) and the melting points (T_m) were determined using a DuPont differential thermal analyzer (DTA, 900) connected to an IBM computer PC/2 and a Hewlett-Packard Colour Pro plotter. The heating rate was 5°C/min and the temperature range was from −50°C to T_m +20°C. The calibration of temperature and heat enthalpy (J/g) of the DTA were made with indium. Five measurements were recorded per sample. Glass transitions (T_g's) were defined as the midpoints of step changes in heat capacities (ΔC_p); melting points and crystallization temperatures were defined as the peaks.

Dynamic Mechanical Thermal Analysis (DMTA) Measurements

DMTA measurements were carried out using a PL-DMTA (MarkII, UK) connected to an Olivetti PC286 and a Hewlett-Packard Colour Pro Plotter. The heating rate was 5°C/min; frequency, 1 Hz, and dimensions of the bars, 40 mm long, 7 mm wide, and 3.2 mm thick. Five measurements were recorded per sample. Tan δ ($= E''/E'$) and E'' (loss modulus) were defined as the peaks of the curves, whereas E' (storage modulus) was defined by the intersection of the extrapolations of the two linear parts.

Wide-angle X-Ray Diffraction Patterns (WAXDP)

WAXDP (2θ = 5–35°) were recorded using a Philips PW1050 diffractometer. Measurements were taken at intervals of 0.05° with a counting time of 4 s. Five measurements were recorded per sample to ensure the reproducibility of our results.

Mechanical Properties

The tensile tests were conducted on a 5 ton Instron universal testing machine (TM-SM 1102, UK). The extension rate was maintained at 1 mm/s. The load elongation curves were plotted and tensile modulus, tensile strength, tensile stress, and percentage strain were calculated from the curves. Compression tests

were also carried out and the crushing load was recorded for the evaluation of the compressive strength. The tensile specimens were of the following geometry: 6 mm width, 30 mm length, and 5 mm thickness, whereas the dimensions of the compressive specimens were 8 mm diameter and 32 mm height. A minimum of five measurements was recorded per sample.

RESULTS AND DISCUSSION

Determination of the Matrix Crystallinity of (Co)polyamide Composites

Wide-angle X-Ray Diffraction Patterns (WAXDP)

Although there exist several well-developed theories for studying the degree of crystallinity of semicrystalline polymers with WAXD,[27-31] the percentage crystallinity of the matrices was only recently investigated. In this field, there is an excellent research work carried out by Spahr and Schultz (who applied the Vonk's theory) on the determination of percentage crystallinity of poly(aryl ether ether ketone)–carbon fiber composites with X-ray diffraction.[3]

The integrated total intensity Q of the X-rays scattered by a semicrystalline polymer reinforced with glass fiber can be expressed in terms of a sum of integrated intensities of the three contributing patterns:

$$Q = Q_{amor} + Q_{cryst} + Q_{fiber} \quad (1)$$

where Q_{amor} is the integrated intensity of the amorphous phase; Q_{cryst}, the integrated intensity of the crystalline phase; and Q_{fiber} is the integrated intensity of the E-glass fiber.

The theoretical corrections of Vonk's equation[28] suggested by Spahr and Schultz[3] were taken into account and, concisely, the idea was to take the diffraction pattern of the amorphous polymer (quenched in liquid nitrogen), of the totally crystalline (100%) polymer, and of the reinforced phase (E-glass fiber), scale them, and add them together to form a composite pattern. However, this model has to allow for several approximations and assumptions, the most important of which are mentioned below:

(a) Since it is virtually impossible to obtain a 100% crystalline (co)polyamide, the crystalline pattern is simulated by summing a series of peaking curves.[3]

(b) The glass fiber-reinforced (co)polyamides are assumed to be completely randomly oriented, which is not always the case for glass fiber (co)polyamide composites.

(c) In one of the several equations involved, there is the assumption that the defects and vibrations associated with one atom are independent of the other atoms,[3] which is not true especially in polymers.

Figures 1 and 2 show the curves of neat nylon 12 50/50 mol/mol CL/LL, amorphous nylon 12, and 50/50 mol/mol CL/LL (quenched in ice water), E-glass fibers, and the composite (glass fiber with nylon 12 and 50/50 mol/mol CL/LL, respectively). Both the neat nylon 12 and 50/50 mol/mol CL/LL patterns and their corresponding glass fiber composites were fit by simulating the major peaks within the range 5°–35°. The results of these calculations are shown in Figures 1 and 2 by the term "calculated nylon 12 or 50/50 mol/mol CL/LL reinforced with glass fiber." Although Figures 1 and 2 may present the drawbacks of this method more intensely than they actually are, they give an overall view of the different diffraction spectra involved in the spectra of the (co)polyamide composites. The results of

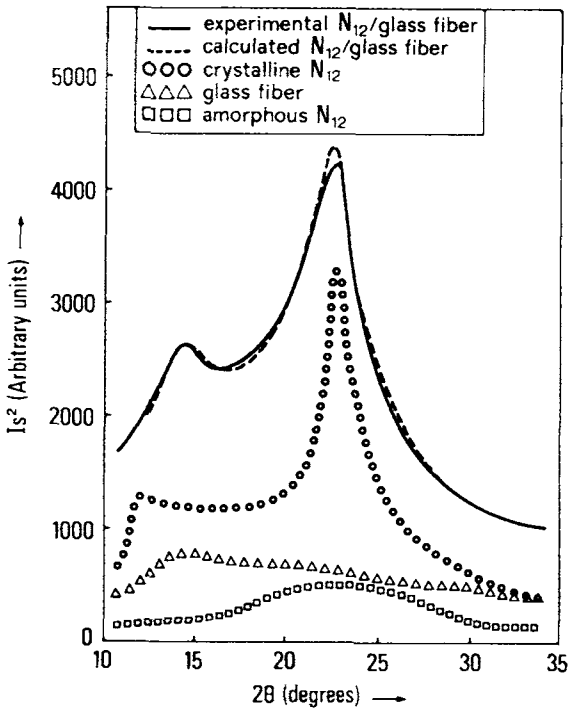

Figure 1 Comparison of experimental and calculated diffraction patterns for E-glass fiber reinforced nylon 12.

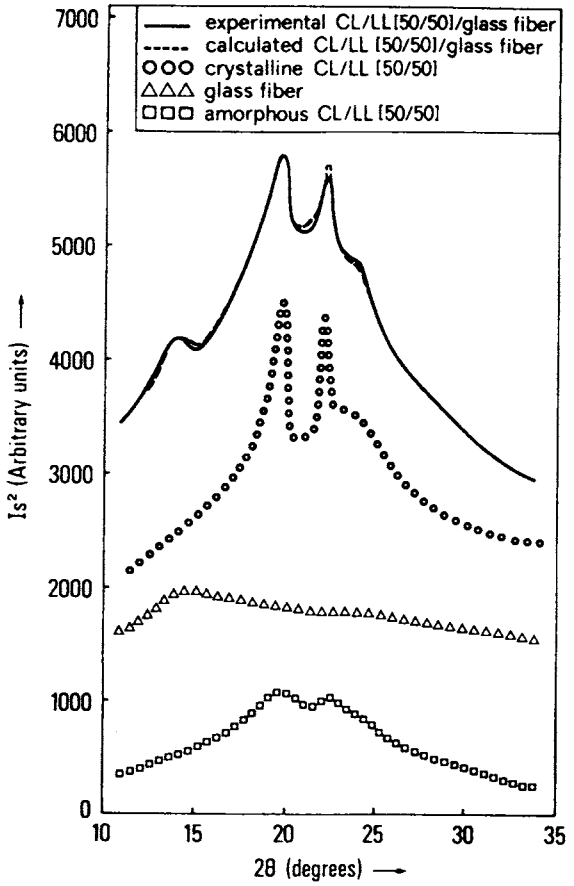

Figure 2 Comparison of experimental and calculated diffraction patterns for E-glass fiber-reinforced (co)polyamide 50/50 mol/mol CL/LL.

percentage crystallinity obtained from this method both for neat and the glass fiber-reinforced (co)polyamides are given in Table I.

Although the drawbacks of this method for determining the percentage crystallinity of the composite matrix have been reported, there are also several important advantages worthy to be mentioned in support of this method:

(a) No knowledge of weight fraction of the polymer in the polymer composite is required.

(b) WAXDP are self-scaling, whereas in thermal methods (differential thermal analysis, DTA), extrapolations to the 100% crystalline polymer are required.

(c) The presence of defects in crystals is taken into account in a reasonable way.

Differential Thermal Analysis (DTA)

Although the utilization of DTA in neat polymers (not containing fillers or fibers) is a rather straightforward technique despite its inadequacies,[32] its application to composite materials is further complicated by the presence of filler or fiber (as in our case) that may give rise to a different model of crystallization. Indeed, apart from the development of spherulites occurring via a statistical nucleation process in the melt, the presence of such a considerable surface like the glass fiber could initiate additional nucleation fronts that occur mainly on the glass fiber. This phenomenon is widely known as transcrystallinity. Figure 3 shows diagrammatically the two morphologies, which have been confirmed for carbon-filled PEEK, PEK, and PPS samples,[34] which might also be applicable to our glass fiber-reinforced (co)polyamides. When the glass fibers are far apart and the matrix is characterized by high nucleating density, transcrystalline layers are expected to grow out at right angles to the glass fiber direction [Fig. 3(a)]. On the contrary, when the glass fibers are very closely packed together, the

Table I Percentage Crystallinity (%X_c) of Polyamides Reinforced with Glass Fiber with Wide-Angle X-ray Diffraction Pattern (WAXDP)

CL/LL (mol/mol)	% Glass-fibre Content	% X_c
0/100	0	28.1
	15	31.0
	30	33.8
	45	36.5
25/75	0	18.7
	15	21.2
	30	24.3
	45	26.4
50/50	0	15.0
	15	16.2
	30	17.5
	45	19.4
75/25	0	26.0
	15	29.2
	30	31.3
	45	33.5
100/0	0	36.7
	15	38.9
	30	41.2
	45	43.4

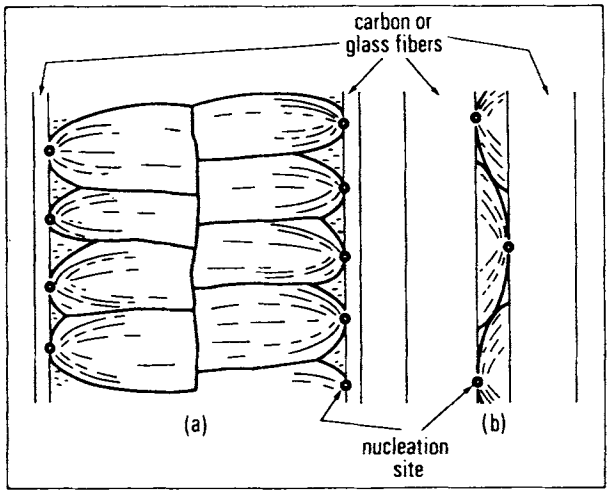

Figure 3 Diagrammatic representation of the two possible spherulite morphologies[33] resulting from constrained growth in thermoplastic composites: (a) high nucleating density; (b) low nucleating density.

growth of spherulites is very limited and possible only along directions parallel to the glass fiber [Fig. 3(b)].

The glass transitions (T_g), melting points (T_{m1}, T_{m2}, and, occasionally, T_{m3}), heats of melting (ΔH_m), and percentage crystallinities ($\%X_c$) of the composites for glass fiber-reinforced (co)polyamides of different compositions and for different cooling rates are given in Tables I–III.

In the polyamide composites consisting of the homopolyamides (nylon 6 or nylon 12) and the E-glass fiber, two peaks (endotherms) were observed, whereas in the neat homopolymers, there was only one melting peak (Fig. 4). Similarly, three peaks were recorded for the (co)polyamide (50/50) composite, whereas the two peaks for the neat (50/50) (co)polyamide should be attributed to different morphologies.[18] This opinion was corroborated by the observation that the lower melting peak did not appear to be a shoulder of the higher melting peak for the homopolymer composites[34] (Fig. 4). The reported higher, among the two, melting peak of the homopolymer composite, occurring at higher temperatures than the T_m of the neat homopolymer, has been previously attributed to the presence of the above-mentioned transcrystalline layers, because the latter form at higher temperatures during cooling due to high nucleation rates.[34] The presence of two

Table II Thermal Properties (Glass Transition [T_g], Melting Points [T_m], Heats of Melting [ΔH_m] and Percentage Crystallinity ($\%X_c$) According to Heats of Melting (DTA) for Glass Fiber-reinforced (Co)polyamides; Results Give the Average and Standard Deviation of Five Measurements ($x \pm$ SD)

CL/LL mol/mol	% Glass Fiber Content	T_g (°C)	T_{m1} (°C)	T_{m2} (°C)	T_{m3} (°C)	ΔH_m (J/g)	% X_c
0/100	0	40.5 ± 1.0	174.8 ± 1.2	—	—	69.5 ± 1.3	30.9
	15	42.0 ± 0.8	177.0 ± 0.6	157.2 ± 0.6	—	75.2 ± 1.6	33.4
	30	43.8 ± 0.6	181.3 ± 0.9	163.0 ± 1.3	—	80.3 ± 2.1	35.7
	45	45.3 ± 1.0	184.8 ± 1.4	168.0 ± 0.9	—	87.5 ± 1.9	38.9
25/75	0	31.8 ± 0.6	158.3 ± 1.0	141.7 ± 0.7	—	47.8 ± 0.8	22.1
	15	33.0 ± 0.5	162.4 ± 0.9	143.8 ± 1.0	127.3 ± 1.0	54.1 ± 0.7	25.0
	30	34.5 ± 0.7	166.0 ± 0.8	147.0 ± 1.0	131.0 ± 0.8	59.5 ± 0.9	27.5
	45	35.8 ± 0.8	171.0 ± 0.7	150.2 ± 0.9	135.4 ± 0.7	66.7 ± 1.3	30.8
50/50	0	23.4 ± 0.4	146.2 ± 0.9	133.5 ± 0.5	—	34.3 ± 0.5	16.5
	15	25.2 ± 0.6	148.0 ± 0.6	136.1 ± 0.4	120.2 ± 0.3	38.1 ± 0.6	18.3
	30	27.0 ± 0.5	150.6 ± 0.9	140.2 ± 0.6	124.5 ± 0.6	42.6 ± 0.7	20.5
	45	28.4 ± 0.7	153.0 ± 1.0	143.0 ± 0.6	127.2 ± 0.6	50.3 ± 0.9	24.2
75/25	0	35.1 ± 0.6	181.3 ± 0.7	162.0 ± 0.8	—	55.9 ± 1.3	28.0
	15	37.0 ± 1.0	184.5 ± 1.0	165.7 ± 0.9	139.2 ± 0.4	61.5 ± 1.5	30.8
	30	38.3 ± 1.2	188.0 ± 0.9	168.3 ± 0.7	142.4 ± 0.5	66.6 ± 1.7	33.4
	45	39.8 ± 0.6	193.1 ± 1.0	170.9 ± 0.9	145.8 ± 0.7	72.2 ± 2.0	36.2
100/0	0	52.3 ± 0.5	224.5 ± 1.6	—	—	82.0 ± 2.0	42.9
	15	53.7 ± 0.6	226.0 ± 0.8	173.2 ± 0.9	—	85.0 ± 1.8	44.5
	30	54.9 ± 0.5	228.4 ± 1.0	180.4 ± 0.8	—	91.3 ± 2.3	47.8
	45	56.3 ± 0.8	230.2 ± 2.0	188.0 ± 1.1	—	97.4 ± 1.5	51.0

Table III Heats of Melting (ΔH_m) and Percentage Crystallinities (% X_c) of Glass Fiber-reinforced (Co)polyamides (Nylon 6/Nylon 12) with Relation to Different Cooling Rates; Results Give the Average and the Standard Deviation of Five Measurements ($x \pm$ SD)

		Ice Water		Air-cooled		Oven-cooled	
CL/LL (mol/mol)	% Glass Fiber Content	ΔH_m (J/g)	% X_c	ΔH_m (J/g)	% X_c	ΔH_m (J/g)	% X_c
0/100	0	56.7 ± 0.9	25.2	69.5 ± 1.3	30.9	76.1 ± 1.1	33.8
	15	59.4 ± 1.2	26.4	75.2 ± 1.6	33.4	83.0 ± 1.3	36.9
	30	62.3 ± 0.8	27.7	80.3 ± 2.1	35.7	91.6 ± 0.9	40.7
	45	65.3 ± 1.0	29.0	87.5 ± 1.9	38.9	99.0 ± 1.0	44.0
25/75	0	37.0 ± 0.7	17.1	47.9 ± 0.8	22.1	55.4 ± 0.9	25.6
	15	40.0 ± 0.6	18.5	54.1 ± 0.7	25.0	65.4 ± 1.1	30.2
	30	43.7 ± 0.8	20.2	59.5 ± 0.9	27.5	75.3 ± 1.2	34.8
	45	50.7 ± 0.9	23.4	66.7 ± 1.3	30.8	80.5 ± 1.0	37.2
50/50	0	23.9 ± 0.6	11.5	34.3 ± 0.5	16.5	42.4 ± 0.7	20.4
	15	27.5 ± 0.5	13.2	38.1 ± 0.6	18.3	47.6 ± 0.9	22.9
	30	32.9 ± 0.8	15.8	42.6 ± 0.7	20.5	54.1 ± 1.0	26.0
	45	38.1 ± 0.7	18.3	50.3 ± 0.9	24.2	62.0 ± 0.8	29.8
75/25	0	43.9 ± 1.0	22.0	55.9 ± 1.3	28.0	68.4 ± 0.9	32.9
	15	51.8 ± 1.1	24.9	61.5 ± 1.5	30.8	75.7 ± 1.2	36.4
	30	57.2 ± 0.9	27.5	66.6 ± 1.7	33.4	80.1 ± 1.2	38.5
	45	64.1 ± 1.0	30.8	72.2 ± 2.0	36.2	85.7 ± 1.3	41.2
100/0	0	65.3 ± 1.3	34.2	82.0 ± 2.0	42.9	87.9 ± 1.6	46.0
	15	71.6 ± 1.5	37.5	85.0 ± 1.8	44.5	97.1 ± 2.0	50.8
	30	78.0 ± 1.2	40.8	91.3 ± 2.3	47.8	102.4 ± 1.7	53.6
	45	86.1 ± 1.6	44.3	97.4 ± 1.5	51.0	108.9 ± 1.8	57.0

melt endotherms has been also reported for other thermoplastic composites consisting of homopolymers such as PEK,[33] PPS,[34] PEEK,[35] PEKK,[35] and commercial polyamides.[36]

The broad upper peak of the glass fiber-reinforced polyamides should, rather, be attributed to the homopolyamide (nylon 6 or nylon 12) initially laid down (primary nucleation) and the lower peak to secondary nucleation occurring among the initial lamellae. This view is supported by previous work on nylon 6.6 where the occurrence of two melting peaks was attributed to thermodynamically and kinetically favored crystal formation.[37] However, this requires additional experimentation with optical and, preferably, electron scanning microscopy in order to substantiate such a hypothesis.

Finally, the developed percentage crystallinity was also investigated in terms of different cooling rates. In particular, it was found, as it can be seen from Table III, that slow cooling rates produced higher percentage crystallinities, whereas fast cooling rates (quenching) reduced considerably the percentage crystallinity.

Density Measurements—Detection of Void Formation

The density measurements were carried out, first, to determine the percentage crystallinity (and compare it to the WAXDP and DTA measurements) and, second, to determine the void volume fraction. The voids in polymer composites have been attributed to several factors, such as entrapment of air within compounded pelletized material, residual moisture or solvents, release of volatiles due to cure, and shrinkage of restraint volume of the core region.[38,39] The void volume fraction (v) was calculated from the measured (p) and calculated (p_{calcd}) composite densities as follows:

$$v = 1 - \frac{p}{p_{calcd}} \qquad (2)$$

The solid, void-free density of the composite ($p_{compos.}$) was calculated from the density of the pure (co)polyamide (p_p) and that of the glass fiber (p_f):

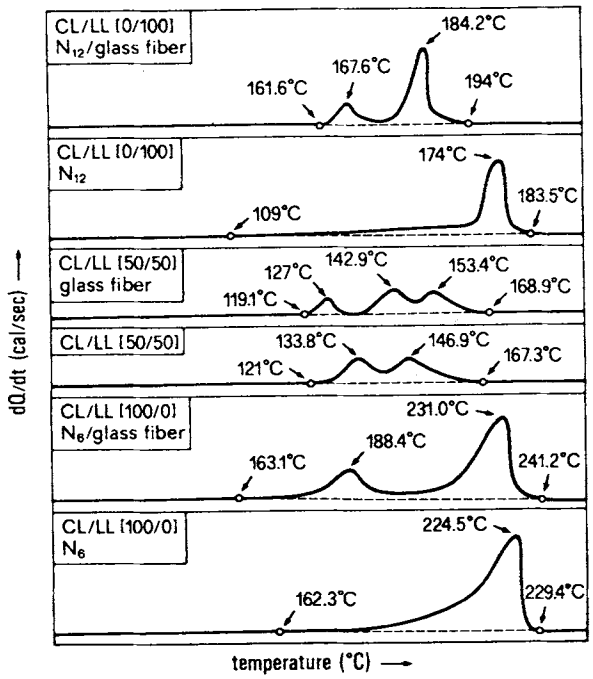

Figure 4 DTA trace for the following neat polymers and their glass fiber composites: (a) neat nylon 6; (b) composite nylon 6; (c) neat 50/50 mol/mol CL/LL; (d) composite 50/50 mol/mol CL/LL; (e) neat nylon 12; (f) composite nylon 12.

$$\frac{1}{p_{\text{compos.}}} = (1 - w)p_p + \frac{w}{p_f} \qquad (3)$$

where w is the glass fiber weight fraction (determined by burning off the (co)polyamide).

The crystallinity ($\%X_c$) of the homopolymers (nylon 6 and nylon 12) were determined according to the following formula:

$$\%X_c = \frac{p_{\text{c.compos.}}(p - p_{\text{a.compos.}})}{p(p_{\text{c.compos.}} - p_{\text{a.compos.}})} \times 100 \qquad (4)$$

where $p_{\text{c.compos.}}$ is the density of the crystalline composite; $p_{\text{a.compos.}}$, the density of the amorphous composite; and p, the measured density. The density of the crystalline composite was calculated as follows:

$$p_{\text{c.compos.}} = \{wp_f + [100 - (v + w)]p_{\text{n.c.p.}}\}/100 \qquad (5)$$

where $p_{\text{n.c.p.}}$ is the density of the neat (100%) crystalline polyamide. Similarly, the density of the amorphous composite was

$$p_{\text{a.compos.}} = \{wp_f + [100 - (v + w)]p_{\text{n.a.p.}}\}/100 \qquad (6)$$

where $p_{\text{n.a.p.}}$ is the density of the neat (100%) amorphous polyamide. Therefore, by substituting eqs. (5) and (6) to eq. (4), we get

$$\%X_c = \frac{[wp_f + (100 - v - w)p_{\text{n.c.p.}}] \times \{100p - [wp_f + (100 - v - w)p_{\text{n.a.p.}}]\}}{p\{[(100 - v - w)p_{\text{n.c.p.}}] - [(100 - v - w)p_{\text{n.a.p.}}]\}} \qquad (7)$$

Table IV gives the density values of the neat (co)polyamides and their fiber-reinforced composites and the void volume fraction developed at different cooling rates. The percentage crystallinities determined from density measurements are given with the values determined from DTA and WAXDP measurements in Table I. Table IV shows that the void volume fraction increases with an increase in glass fiber content, which is in agreement with the results of previous investigations on poly(phenylene oxide)–polystyrene (PPO/PS)/glass fiber[4] and mica-reinforced polystyrene (PS).[38]

Although several of the above-mentioned factors have been occasionally identified as responsible for initiating the void formation, it is recognized that the formation of bubbles is usually the main reason.[40] The bubble formation was described in terms of nucleation and growth in a viscous medium and was found to depend upon the following factors[41]:

(a) diffusivity and concentration of the gas;
(b) viscosity of the polymer melt;
(c) temperature and pressure; and
(d) cooling rate.

An attempt was made to study the effect of the cooling rate upon the void formation in glass fiber-reinforced (co)polyamides (nylon 6/nylon 12). The following three modes of cooling were selected: quenching in ice water, cooling in the air, and cooling gradually in the oven. The effect of these cooling modes on the density and void volume fraction are shown in Figures 5 and 6. The higher void contents from Figures 5 and 6 are as follows: quenching in ice water > air-cooled > oven-cooled.

The promotion of higher void contents with quenching in ice water, compared to the other two cooling modes, could be attributed, as previously,[4] to the initial solidification of the external surface layers that act against the contraction of the inner zones, thus resulting in higher internal void contents. It should be mentioned that the glass-reinforced (co)polyamides of intermediate composition

Table IV Effect of Cooling Conditions on Density (p), Percentage Crystallinity (% X_c) and Void Fraction (u) of Glass Fiber-reinforced (Co)polyamides (Nylon 6/Nylon 12); Results Give the Average and the Standard Deviation of Five Measurements ($x \pm SD$)

CL/LL (mol/mol)	$P_{n.a.p.}$ (g/cm^3)	$P_{n.c.p.}$ (g/cm^3)	% Glass Fiber Content (w)	$P_{c.compos.}$[a] (g/cm^3)	$P_{a.compos.}$[b] (g/cm^3)	Density (g/cm^3) (p)	Void Fraction (v)[c]	% X_c[d]
Ice water								
0/100 or nylon 12	0.972	1.037	0	1.03285	0.96811	$0.9872 \pm 2.1 \times 10^{-4}$	0.004	30.8 ± 1.0
			15	1.21003	1.15816	$1.1748 \pm 3.2 \times 10^{-4}$	0.052	33.0 ± 0.8
			30	1.40483	1.36472	$1.3787 \pm 3.3 \times 10^{-4}$	0.083	35.6 ± 1.1
			45	1.53534	1.51103	$1.5202 \pm 3.0 \times 10^{-4}$	0.176	37.9 ± 1.2
25/75	1.001	1.078	0	1.07261	0.99599	$1.0098 \pm 2.2 \times 10^{-4}$	0.005	19.2 ± 0.8
			15	1.25891	1.19631	$1.2092 \pm 2.4 \times 10^{-4}$	0.037	21.5 ± 0.7
			30	1.45492	1.40564	$1.4169 \pm 2.9 \times 10^{-4}$	0.060	23.4 ± 1.0
			45	1.58732	1.55591	$1.5646 \pm 3.5 \times 10^{-4}$	0.142	28.2 ± 1.2
50/50	1.029	1.129	0	1.12787	1.02797	$1.0414 \pm 1.8 \times 10^{-4}$	0.001	14.5 ± 0.6
			15	1.30376	1.22216	$1.2351 \pm 2.0 \times 10^{-4}$	0.034	16.7 ± 0.9
			30	1.49659	1.43179	$1.4440 \pm 2.3 \times 10^{-4}$	0.052	19.5 ± 0.8
			45	1.62168	1.57968	$1.5884 \pm 2.4 \times 10^{-4}$	0.130	21.3 ± 1.0
75/25	1.058	1.179	0	1.17428	1.05377	$1.0811 \pm 1.1 \times 10^{-4}$	0.004	24.6 ± 1.3
			15	1.34221	1.24371	$1.2703 \pm 1.3 \times 10^{-4}$	0.036	28.5 ± 1.5
			30	1.53253	1.45376	$1.4780 \pm 1.4 \times 10^{-4}$	0.049	31.9 ± 1.6
			45	1.63914	1.58869	$1.6057 \pm 1.6 \times 10^{-4}$	0.133	34.5 ± 2.0
100/0 or nylon 6	1.087	1.220	0	1.21024	1.07830	$1.1262 \pm 1.8 \times 10^{-4}$	0.008	39.0 ± 1.5
			15	1.36338	1.25645	$1.3000 \pm 2.5 \times 10^{-4}$	0.046	42.7 ± 2.1
			30	1.52750	1.44438	$1.4806 \pm 3.0 \times 10^{-4}$	0.075	44.9 ± 2.3
			45	1.63184	1.57904	$1.6039 \pm 3.3 \times 10^{-4}$	0.153	47.8 ± 2.6
Oven-cooled								
0/100 or nylon 12	0.972	1.037	0	1.03493	0.97006	$0.9930 \pm 2.0 \times 10^{-4}$	0.020	36.8 ± 1.4
			15	1.23491	1.18148	$1.2028 \pm 2.3 \times 10^{-4}$	0.028	41.0 ± 1.9
			30	1.45046	1.40750	$1.3818 \pm 2.4 \times 10^{-4}$	0.039	45.9 ± 2.2
			45	1.61208	1.58296	$1.5974 \pm 2.6 \times 10^{-4}$	0.102	50.1 ± 2.6
25/75	1.001	1.078	0	1.07800	1.00100	$1.0222 \pm 1.8 \times 10^{-4}$	0.001	29.0 ± 1.1
			15	1.27616	1.21233	$1.2338 \pm 2.1 \times 10^{-4}$	0.021	34.8 ± 1.6
			30	1.47756	1.42666	$1.4462 \pm 2.4 \times 10^{-4}$	0.039	39.3 ± 1.8
			45	1.62721	1.59295	$1.6071 \pm 2.6 \times 10^{-4}$	0.105	41.7 ± 2.5

50/50	1.029	1.129	0	1.12787	1.02797	$1.0518 \pm 1.7 \times 10^{-4}$	0.001	25.6 ± 1.3
			15	1.32522	1.24172	$1.2636 \pm 2.0 \times 10^{-4}$	0.015	27.5 ± 1.4
			30	1.51917	1.45237	$1.4726 \pm 2.3 \times 10^{-4}$	0.032	31.2 ± 2.0
			45	1.66797	1.62187	$1.6380 \pm 2.4 \times 10^{-4}$	0.089	35.6 ± 2.2
75/25	1.058	1.179	0	1.17782	1.05694	$1.0991 \pm 1.0 \times 10^{-4}$	0.001	37.4 ± 2.3
			15	1.36461	1.26381	$1.3039 \pm 1.1 \times 10^{-4}$	0.017	41.6 ± 2.9
			30	1.55493	1.47386	$1.5084 \pm 1.4 \times 10^{-4}$	0.030	43.9 ± 3.2
			45	1.68866	1.63312	$1.6578 \pm 1.5 \times 10^{-4}$	0.091	45.3 ± 3.4
100/0 or nylon 6	1.087	1.220	0	1.21756	1.08483	$1.1476 \pm 1.2 \times 10^{-4}$	0.002	50.2 ± 3.6
			15	1.38778	1.27819	$1.3357 \pm 1.3 \times 10^{-4}$	0.026	54.5 ± 3.7
			30	1.57630	1.48786	$1.5381 \pm 1.6 \times 10^{-4}$	0.035	58.2 ± 3.8
			45	1.69406	1.63448	$1.6706 \pm 1.5 \times 10^{-4}$	0.102	61.5 ± 3.7
Air-cooled								
0/100 or nylon 12	0.972	1.037	0	1.03596	0.97103	$0.9929 \pm 2.5 \times 10^{-4}$	0.001	35.2 ± 1.4
			15	1.22766	1.17468	$1.1952 \pm 3.3 \times 10^{-4}$	0.035	39.8 ± 1.7
			30	1.43905	1.39680	$1.4142 \pm 3.7 \times 10^{-4}$	0.050	42.0 ± 2.0
			45	1.57786	1.55088	$1.5629 \pm 3.8 \times 10^{-4}$	0.135	44.9 ± 2.4
25/75	1.001	1.078	0	1.07584	0.99900	$1.0172 \pm 2.1 \times 10^{-4}$	0.002	25.0 ± 1.3
			15	1.27077	1.20732	$1.2250 \pm 2.3 \times 10^{-4}$	0.026	28.9 ± 1.6
			30	1.46893	1.41865	$1.4343 \pm 2.7 \times 10^{-4}$	0.047	31.8 ± 1.8
			45	1.60996	1.57692	$1.5882 \pm 3.2 \times 10^{-4}$	0.121	34.5 ± 1.9
50/50	1.029	1.124	0	1.12787	1.02797	$1.0459 \pm 2.7 \times 10^{-4}$	0.001	19.4 ± 1.2
			15	1.31957	1.23657	$1.2538 \pm 3.6 \times 10^{-4}$	0.020	21.8 ± 1.3
			30	1.50562	1.44002	$1.4558 \pm 3.8 \times 10^{-4}$	0.044	24.9 ± 1.5
			45	1.64990	1.60541	$1.6189 \pm 4.2 \times 10^{-4}$	0.105	28.6 ± 1.7
75/25	1.058	1.179	0	1.17664	1.05588	$1.0912 \pm 2.2 \times 10^{-4}$	0.002	31.5 ± 2.0
			15	1.35871	1.25852	$1.2916 \pm 2.7 \times 10^{-4}$	0.022	34.7 ± 2.1
			30	1.54550	1.46540	$1.4948 \pm 3.3 \times 10^{-4}$	0.038	38.0 ± 2.3
			45	1.66626	1.61302	$1.6347 \pm 3.6 \times 10^{-4}$	0.110	41.5 ± 2.4
100/0 or nylon 6	1.087	1.220	0	1.21390	1.08157	$1.1381 \pm 1.8 \times 10^{-4}$	0.005	45.6 ± 2.6
			15	1.38168	1.27275	$1.3236 \pm 2.9 \times 10^{-4}$	0.031	48.7 ± 2.7
			30	1.56410	1.47699	$1.5210 \pm 3.3 \times 10^{-4}$	0.045	51.9 ± 2.8
			45	1.67210	1.61491	$1.6470 \pm 3.8 \times 10^{-4}$	0.120	57.0 ± 3.2

[a] Calculated according to eq. (5).
[b] Calculated according to eq. (6).
[c] Calculated according to eq. (2).
[d] Calculated according to eq. (7).

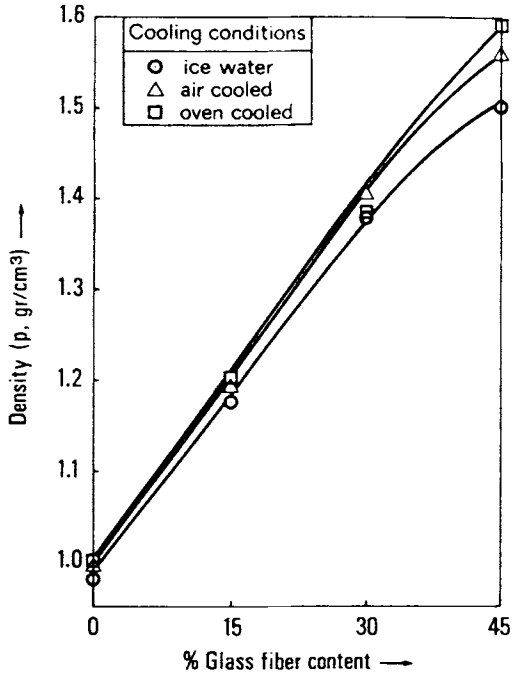

Figure 5 Effect of cooling conditions on density vs. the glass fiber concentration of glass fiber-reinforced nylon 12.

(i.e., 50/50 mol/mol CL/LL) exhibit a lesser formation of void volume fraction than do the homopolyamides (nylon 6 and nylon 12). This could be attributed to the fact that the intermediate composition (co)polyamides are of lower viscosity (than that of the homopolyamides because of their lower MW) and, therefore, of greater mobility and less proned to the formation of bubbles that may eventually lead to void formation.

Mechanical Properties

Tensile Strength

Typical stress–strain curves showing the effect of the glass fiber upon the stress of the (co)polyamide (nylon 6/nylon 12) composites were recorded at room temperature. An increase in the glass fiber content showed a gradual increase in the tensile strength of the (co)polyamide composites.

The most interesting feature of the stress–strain curves was the lack of any yielding point for the (co)polyamide composites, whereas the neat (co)polyamides (nylon 6/nylon 12) showed definite yield points before their fracture. The slope of the curves, varied according to the (co)polyamide composition, remained constant up to 10% of strain before being reduced to the point of fracture. Tables V and VI summarize all the results derived both from the stress–strain curves and the compressive strength–time (distance) plots for the neat and the composite (co)polyamides.

The simplest way to proceed to the analysis of the tensile strength of glass fiber-reinforced (co)polyamides is to apply the rule of mixtures[20,42] (provided that matrix and glass fiber are of the same Poisson's number)[43]; i.e.:

$$\sigma_u = n\sigma_f V_f + \sigma_m(1 - V_f) \tag{8}$$

where σ_u is the tensile strength of the composite; σ_f, the tensile strength of the glass fiber; σ_m, the tensile strength of the matrix (in our case (co)polyamide); V_f, the fiber volume fraction; and n, the Krenchel's efficiency factor ($n = 0.5$ for cross-ply fiber composites).[20,27]

On the basis of experimental data and theoretical analysis, Weibull[44] suggested a much more simplified eq. (9) given below, which has been already applied successfully to composites prepared from E-glass fiber and nylon 6.6[20]:

$$\sigma_u = 0.7\sigma_f V_f \tag{9}$$

The statistical analysis of strength of composites (reinforced with fibers) was conducted by Dow and Rosen (cited by Shrivastava and Lal[20]) and resulted in the following formula:

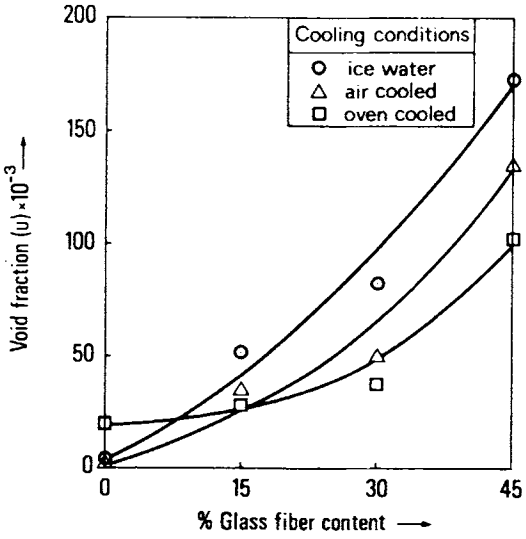

Figure 6 Effect of cooling conditions on void content vs. the glass fiber concentration of glass fiber-reinforced nylon 12.

Table V Theoretical and Experimental Ultimate Tensile Strength Values (MPa) for Copolymide Composites of Different Glass Fiber Contents; Experimental Results Give the Average and the Standard Deviation of Five Measurements ($x \pm SD$)

CL/LL (mol/mol)	% Glass Fiber Content	Experimental	Tensile Strength (MPa)						
			Calculated According to eq. (8)	Calculated According to eq. (9)	Calculated According to Modified eq. (9)	Corrected Multiplication Coefficient Instead of 0.7	Calculated According to eq. (10)	Calculated According to Modified eq. (10)	Corrected Multiplication Coefficient Instead of 0.7
0/100 or nylon 12	0	31.5 ± 1.2	31.5	—	—	—	—	—	—
	15	262.0 ± 3.4	289.3	367.5	236.3	0.45	347.9	238.6	0.48
	22.5	374.5 ± 14.8	418.2	551.3	354.4	0.45	529.2	362.9	0.48
	30	490.6 ± 15.7	547.1	735.0	472.5	0.45	715.4	490.6	0.48
	37.5	613.2 ± 14.5	675.9	918.8	590.6	0.45	904.1	619.9	0.48
	45	701.0 ± 17.0	804.8	1102.5	708.8	0.45	1095.2	751.0	0.48
25/75	0	13.2 ± 0.3	13.2	—	—	—	—	—	—
	15	230.0 ± 5.6	237.7	367.5	236.3	0.45	347.9	233.6	0.47
	22.5	367.5 ± 8.9	404.0	551.3	354.4	0.45	529.2	355.3	0.47
	30	475.6 ± 17.8	534.2	735.0	472.5	0.45	715.4	480.3	0.47
	37.5	612.3 ± 19.7	664.5	918.8	590.6	0.45	904.1	607.0	0.47
	45	725.4	794.8	1102.5	708.8	0.45	1095.2	735.3	0.47
50/50	0	8.9 ± 0.5	8.9	—	—	—	—	—	—
	15	220.3 ± 10.3	270.1	367.5	225.8	0.43	347.9	218.7	0.44
	22.5	335.0 ± 20.4	400.6	551.3	338.6	0.43	529.2	332.6	0.44
	30	443.4 ± 17.0	531.2	735.0	451.5	0.43	715.4	449.7	0.44
	37.5	545.0 ± 13.4	661.8	918.8	564.4	0.43	904.1	568.3	0.44
	45	673.8 ± 20.4	792.4	1102.5	677.3	0.43	1095.2	688.4	0.44
75/25	0	17.6 ± 1.3	17.6	—	—	—	—	—	—
	15	240.8 ± 8.9	277.5	367.5	246.8	0.47	347.9	238.6	0.48
	22.5	382.0 ± 7.5	407.4	551.3	370.1	0.47	529.2	362.9	0.48
	30	494.0 ± 16.0	537.3	735.0	493.5	0.47	715.4	490.6	0.48
	37.5	625.6 ± 17.5	667.3	918.8	616.9	0.47	904.1	619.9	0.48
	45	744.3 ± 20.4	797.2	1102.5	740.3	0.47	1095.2	751.0	0.48
100/0 or nylon 6	0	40.0 ± 0.3	40.0	—	—	—	—	—	—
	15	275.4 ± 12.3	296.5	367.5	262.5	0.50	347.9	253.5	0.51
	22.5	408.5 ± 18.5	424.8	551.3	393.8	0.50	529.2	385.6	0.51
	30	525.8 ± 15.0	553.0	735.0	525.0	0.50	715.4	521.2	0.51
	37.5	638.0 ± 14.2	681.3	918.8	656.3	0.50	904.1	658.7	0.51
	45	765.0 ± 20.0	809.5	1102.5	787.5	0.50	1095.2	797.9	0.51

Table VI Theoretical and Experimental Tensile Moduli Values (GPa) and Compressive Strength (MPa) of Different Glass Fiber Contents; Experimental Results Give the Average and the Standard Deviation of Five Measurements ($x \pm SD$)

		Tensile Modulus (GPa)			Compressive Strength (MPa)				
CL/LL (mol/mol)	% Glass Fiber Content	Experimental	Theoretical Lower Limit According to eq. (15)	Theoretical Upper Limit According to eq. (13)	Experimental	Theoretically Calculated According to eq. (16)	Theoretically Calculated According to eq. (17)	Theoretically Calculated According to Modified eq. (17)	Correction Coefficient Instead of 0.63
0/100 or nylon 12	0	1.15 ± 0.09	—	—	71.4 ± 5.0	—	—	—	—
	15	1.90 ± 0.12	1.35	6.60	106.0 ± 7.0	536.3	741	122.4	0.104
	22.5	2.85 ± 0.25	1.48	9.33	125.6 ± 6.5	1031.9	813	134.2	0.104
	30	4.19 ± 0.38	1.64	12.06	152.0 ± 7.5	1671.6	900	148.6	0.104
	37.5	5.65 ± 0.40	1.84	14.78	185.0 ± 6.0	2472.6	1008	166.4	0.104
	45	6.90 ± 0.45	2.09	18.03	215.9 ± 5.0	3464.6	1145	189.1	0.104
25/75	0	0.80 ± 0.06	—	—	47.5 ± 2.9	—	—	—	—
	15	1.30 ± 0.09	0.94	6.30	68.9 ± 4.1	447.1	497	82.0	0.104
	22.5	2.10 ± 0.30	1.03	9.06	93.4 ± 6.5	860.5	545	89.9	0.104
	30	3.08 ± 0.22	1.14	11.81	110.0 ± 8.0	1394.2	603	99.5	0.104
	37.5	4.20 ± 0.19	1.28	14.56	133.5 ± 6.8	2066.2	675	111.5	0.104
	45	5.37 ± 0.35	1.45	17.32	158.4 ± 8.0	2889.7	767	126.7	0.104
50/50	0	0.50 ± 0.04	—	—	30.0 ± 3.0	—	—	—	—
	15	0.90 ± 0.08	0.59	6.05	52.5 ± 4.2	353.5	296	65.9	0.140
	22.5	1.69 ± 0.13	0.65	8.83	73.0 ± 5.6	680.2	325	72.3	0.140
	30	2.26 ± 0.2	0.71	11.60	95.0 ± 7.2	1102.1	360	80.0	0.140
	37.5	3.35 ± 0.32	0.80	14.38	109.2 ± 8.5	1630.2	403	89.6	0.140
	45	4.59 ± 0.41	0.91	17.15	128.5 ± 10.0	2284.4	458	101.8	0.140
75/25	0	0.95 ± 0.07	—	—	57.5 ± 2.9	—	—	—	—
	15	1.60 ± 0.12	1.12	6.43	78.0 ± 6.5	487.3	578	91.7	0.100
	22.5	2.28 ± 0.09	1.23	9.17	101.5 ± 7.0	937.6	634	100.6	0.100
	30	3.25 ± 0.12	1.36	11.92	123.0 ± 6.0	1519.2	702	111.4	0.100
	37.5	4.41 ± 0.30	1.52	14.66	145.8 ± 11.0	2247.1	786	124.8	0.100
	45	5.82 ± 0.25	1.73	17.40	173.4 ± 15.6	3148.6	893	141.8	0.100
100/0 or nylon 6	0	1.29 ± 0.11	—	—	80.0 ± 4.2	—	—	—	—
	15	2.55 ± 0.30	1.52	6.72	115.5 ± 5.0	597.9	682	129.9	0.120
	22.5	3.60 ± 0.40	1.66	9.44	142.6 ± 4.5	1092.8	748	142.4	0.120
	30	4.75 ± 0.35	1.84	12.15	169.0 ± 7.8	1770.6	828	157.7	0.120
	37.5	6.32 ± 0.40	2.06	14.87	205.6 ± 12.5	2618.7	927	176.6	0.120
	45	7.80 ± 0.30	2.35	17.58	251.0 ± 14.0	3252.4	1054	200.7	0.120

$$\sigma_u = \sigma_r V_f \left[\frac{(1 - V_f)^{0.5}}{V_f^{0.5}} \right]^{-1/2\beta} \quad (10)$$

where σ_r is the reference stress level depending on the particular combination of fiber and matrix ((co)polyamide in our case) properties and β is a statistical parameter of the Weibull distribution related to the fiber strength, which is equal to 7.7 for commercial E-glass fiber.[20]

Our experimental results (Tables V and VI) were compared to the values obtained from these three equations [(8)–(10)]. Figures 7–9 show the predicted values with comparison to those experimentally found. It is obvious that eq. (9) approaches closer to the experimental values, as was also observed in the case of polyamide (nylon 6.6) composites.[20] The discrepancies of the predicted values from eqs. (8) and (10) from the experimental values could be attributed to the hygroscopic (co)polyamide matrix and the void content of the (co)polyamide (nylon 6/nylon 12) composites.[4]

Tensile Modulus

Assuming that the (co)polyamide (nylon 6/nylon 12) glass-reinforced composites are stressed parallel

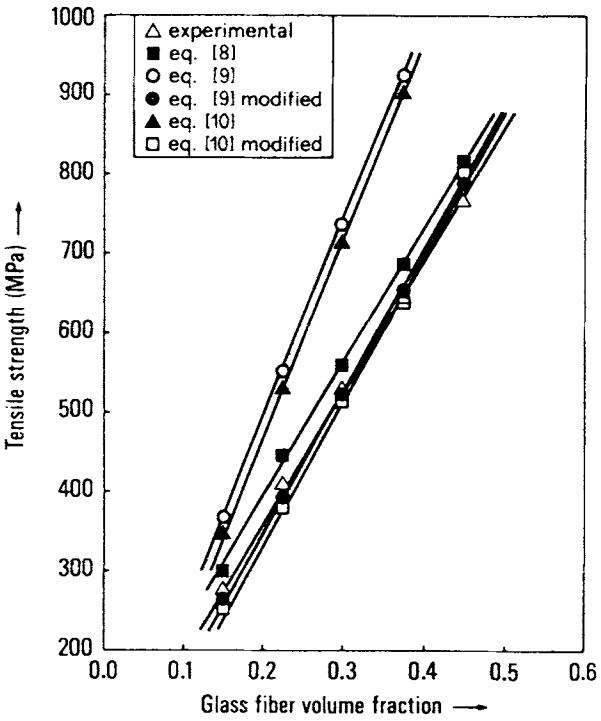

Figure 8 Ultimate tensile strength plotted against glass fiber concentration for glass fiber-reinforced nylon 6.

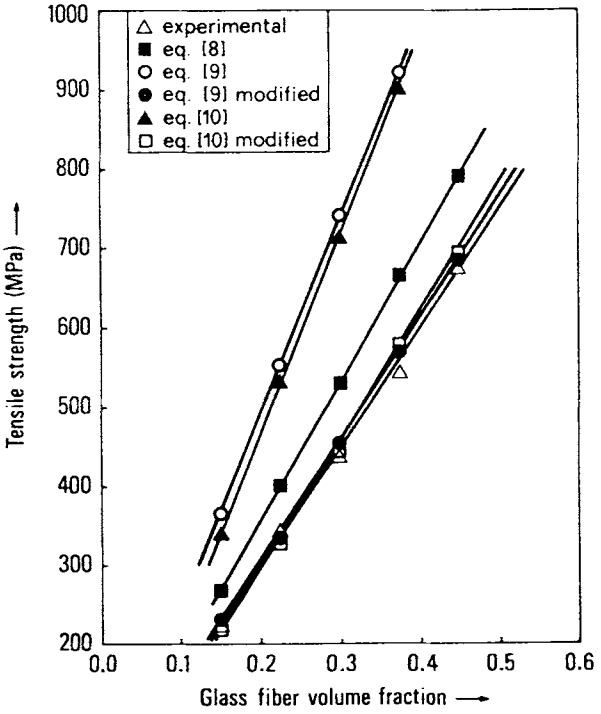

Figure 7 Ultimate tensile strength plotted against glass fiber concentration for glass fiber-reinforced 50/50 mol/mol CL/LL.

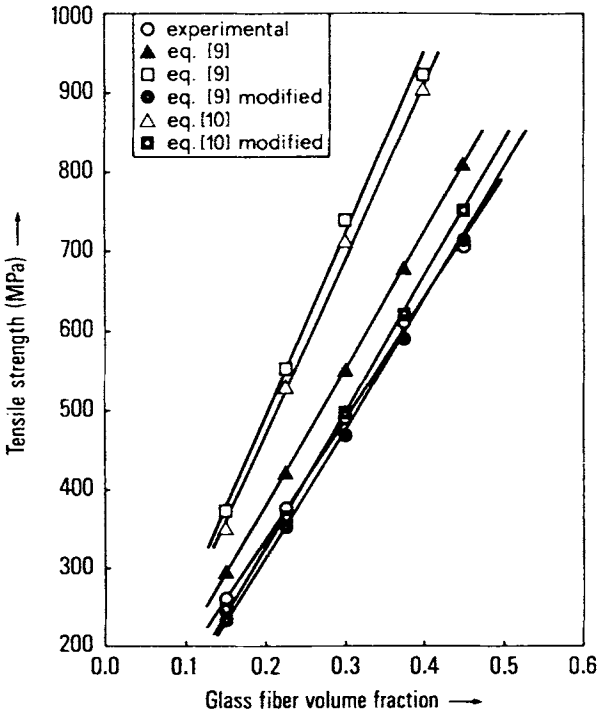

Figure 9 Ultimate tensile strength plotted against glass fiber concentration for glass fiber-reinforced nylon 12.

to the glass fibers and the strains in the glass fibers and (co)polyamide matrices are equal [Fig. 10(a)], it is natural to assume that the strains in the glass fibers and the matrices are equal. Then, the stress carried by the (co)polyamide composite is

$$\sigma = V_f \sigma_f + (1 - V_f)\sigma_m = E_f V_f \varepsilon_n + E_m(1 - V_f)\varepsilon_n \quad (11)$$

But since

$$E_{\text{composite}} = \frac{\sigma}{\varepsilon_n} \quad (12)$$

then a combination of eqs. (11) and (12) gives

$$E_{\text{composite}} = V_f E_f + (1 - V_f)E_m \quad (13)$$

Obviously, this gives the upper estimate for the modulus of the glass fiber-reinforced (co)polyamides. However, if the composite was loaded at right angles to the fiber [Fig. 10(b)], we can assume

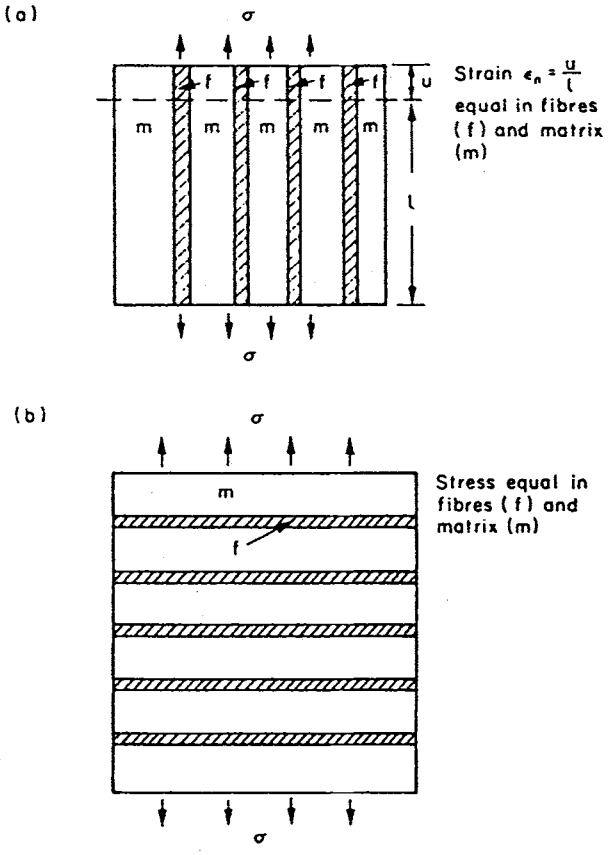

Figure 10 A glass fiber-reinforced (co)polyamide loaded so as to give (a) maximum modulus and (b) minimum modulus after Ashby and Jones.[45]

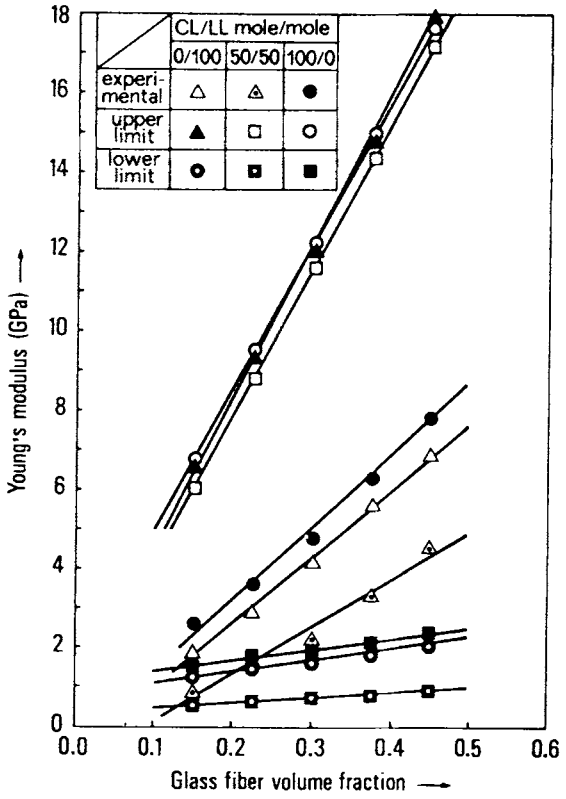

Figure 11 Young's modulus plotted vs. glass fiber concentration for nylon 6 and 50/50 mol/mol CL/LL and nylon 12.

that the stresses of the two components are equal. Therefore, the total nominal strain ε_n is the weighed sum of the individual strains:

$$\varepsilon_n = V_f \varepsilon_{nf} + (1 - V_f)\varepsilon_{nm} = \frac{V_f \sigma}{E_f} + \left(\frac{1 - V_f}{E_m}\right)\sigma \quad (14)$$

Therefore, by substituting eq. (12) in eq. (14), we get

$$E_{\text{composite}} = \frac{1}{\left\{\frac{V_f}{E_f} + \left(\frac{1 - V_f}{E_m}\right)\right\}} \quad (15)$$

Equation (15) gives the lower limit of the modulus.

The upper and lower limits of the Young's (tensile) modulus for nylon 6, nylon 12, and the 75/25, 50/50, and 25/75 mol/mol CL/LL and the experimentally found values are shown for comparison purposes in Figure 11. An increase in the percentage of glass fiber content in the (co)polyamide com-

posites induces an increase in the Young's (tensile) modulus and tensile strength for the composites of different polyamide composition. The obtained results of the Young's (tensile) modulus and tensile strength lie in the following order:

(nylon 6) or 100/0 > (nylon 12) or 0/100

> 75/25 > 25/75 > 50/50 mol/mol CL/LL

where CL = caprolactam monomer for nylon 6 and LL = laurolactam monomer for nylon 12.

The fact that the experimental values are closer rather to the lower theoretically predicted limit was previously attributed to lack of orientation, due to this particular method of preparation, of the (co)polyamide composites.[20] It was also observed that the lowest possible discrepancies between theoretical and experimental values occur at the (co)polyamide composites with the lowest glass fiber content. To investigate the previous assumption that this phenomenon is due to an increase in void content at higher glass fiber volume fractions, a detailed analysis of void content was carried out (see Density Measurements—Detection of Void Formation, above) and its correlation with several mechanical properties was attempted (see Correlation of Mechanical Properties with Percentage Crystallinity and Void Volume Fraction, below).

Compression Strength

Although several models for describing the compressive strength of fiber-reinforced polymer composites have been occasionally suggested,[20] the two most successfully applied equations are as follows:

$$\sigma_{ce} = 2V_f\left[\frac{V_f E_m E_f}{3(1 - V_f)}\right]^{0.5} \quad (16)$$

$$\sigma_{cs} = \frac{G_m}{1 - V_f} \quad (17)$$

where σ_{ce} is the compressive strength in the extension mode; σ_{cs}, the compression strength in the shear mode; E_m, the modulus of the elasticity of the matrix [(co)polyamides]; E_f, the modulus of the elasticity of the fiber (glass fiber); and G_m, the shear modulus.

However, eq. (17) can describe satisfactorily the behavior of (co)polyamides (nylon 6/nylon 12) reinforced with glass fibers only when a correction factor is introduced into the equation. This correction factor was 0.63 for boron–epoxy composites,[46] 0.25 for glass fiber–nylon 6.6 composites,[20] and, in our case, varied from 0.100 to 0.140 depending on the percentage composition of the (co)polyamides. Figures 12 and 13 show schematically the predictions of eqs. (16) and (17), after they have been multiplied with 0.63, the predictions of eq. (17) multiplied with (0.100–0.140), and the experimental values.

Correlation of Mechanical Properties with Percentage Crystallinity and Void Volume Fraction

The presence of voids in the polymer composites has proved to incur a substantial decrease in their mechanical properties (i.e., 4% void content, approximately 30% decrease in the mechanical properties).[4]

If the tensile strength is plotted vs. the void volume fraction, a continuous increase in the tensile strength is observed (Fig. 14) despite the development of greater void contents at higher fiber contents. This behavior (similar results were obtained for the Young's modulus and compressive strength) could be attributed to the development of transcrystallinity that may counteract the void content effect.

Although an increase in the percentage crystallinity generally leads to a decrease in the strain to failure that is attributed to increased brittleness of the polymer with development of crystallinity,[47] the

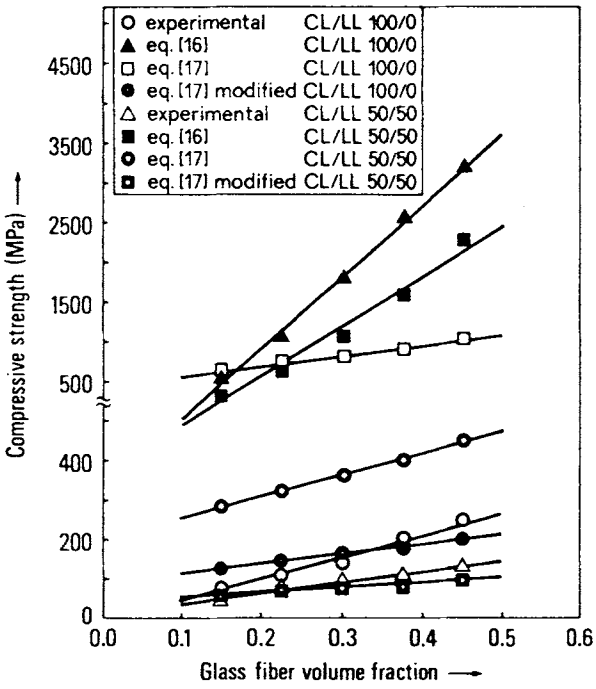

Figure 12 Compressive strength plotted vs. glass fiber concentration for nylon 6 and 50/50 mol/mol CL/LL.

presence of transcrystallinity was found to enhance the interfacial strength between the fibers and the polymeric matrix,[34] provided that the fiber content is less than 60%. Since in our case the maximum fiber content is 45%, it could be suggested that the positive effect of the transcrystallinity counterbalances the negative effect of the increased void content. However, it was found that if the fiber content exceeds the standard 60%, the action of transcrystallinity is reversed by becoming synergistic with the void content. In particular, it was shown that weaknesses may arise at the interfaces between adjacent transcrystalline regions, thereby producing an area ideal for stress and crack propagation.[48]

CONCLUSIONS

The percentage crystallinity of the glass fiber-reinforced (co)polyamides (nylon 6/nylon 12) was determined with three different methods: WAXDP, DTA, and density measurements, which showed satisfactory accord. Several previously suggested models for prediction of the mechanical properties were investigated, and modifications in order to obtain better fit for the experimental results were proposed. The effect of transcrystallinity upon the thermal (creating two crystal morphologies) and mechanical properties [promoting the strength of (co)polyamide composites] was discussed in conjunction with the effect of void content.

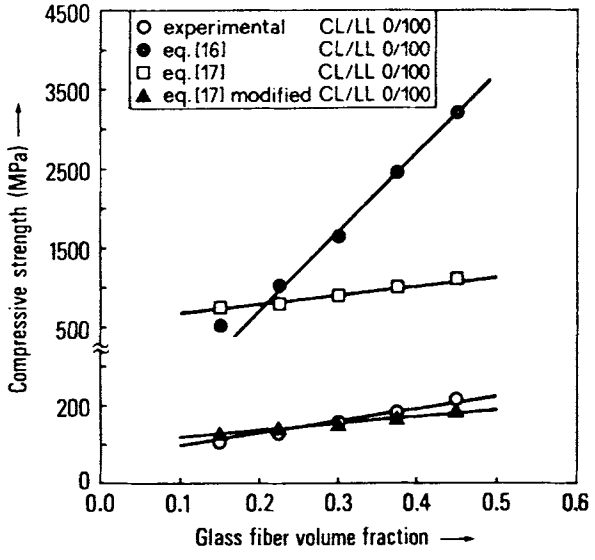

Figure 13 Compressive strength plotted vs. glass fiber concentration for nylon 12.

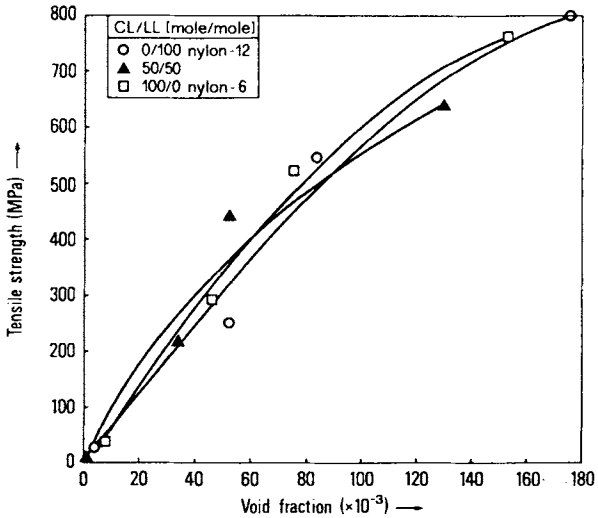

Figure 14 Ultimate tensile strength vs. void content for nylon 6, nylon 12, and 50/50 mol/mol CL/LL.

I. A. is indebted to Professor Blanshard (University of Nottingham, UK) for providing him with all the necessary facilities for this research. I. A. is also grateful to Mrs. Val Street for her technical assistance.

REFERENCES

1. L. N. Philips, *Fabrication in Advanced Composite Materials,* L. N. Philips, Ed., Springer-Verlag, Berlin, New York, London, 1989.
2. D. F. Hiscock and D. M. Bigg, *Polym. Compos.*, **10**(3), 145 (1989).
3. D. E. Spahr and J. M. Schultz, *Polym. Compos.*, **11**(4), 201 (1990).
4. A. Vaxman, M. Narkis, A. Siegman, and S. Kenig, *Polym. Compos.*, **10**(6), 449 (1989).
5. L. N. Philips, in *Proceedings of Salford Symposium on Fabrication Techniques for Advanced Reinforced Plastics,* IPC Science and Technology Press, Guilford, Surrey, 1980, p. 101.
6. C. S. Temple and J. R. Matthews, U.S. Pat. 3,684,645 (Mar. 25, 1969).
7. I. S. Biggs, B. Radvan, and A. J. Willis, *Plastics on the Road '86,* The Plastics and Rubber Institute, London, 1986, p. 41.
8. R. A. Wessling, L. D. Yats, and D. K. Tolbert, U.S. Pat. 4,426,470 (Jan. 17, 1984).
9. A. Vallee and H. Cortinchi, U.S. Pat. 4,645,565 (Feb. 24, 1987).
10. B. R. Bassett and A. F. Yee, *Polym. Compos.*, **11**(1), 10 (1990).
11. D. W. Rosato and C. S. Grove, *Filament Winding,* New York, Wiley-Interscience, New York, 1964.
12. K. J. Iddon and C. Blundell, *Proceedings of Salford Symposium on Fabrication Techniques for Advanced*

Reinforced Plastics, IPC Science and Technology Press, Guiford, Surrey, 1980, p. 58.
13. R. P. Scheldon, *Composite Polymeric Materials,* Applied Science, London, New York, 1982, p. 141.
14. C. Smith and J. Stone, in *Composite Materials Technology,* P. K. Mallick and S. Newman, Eds., Hanser, Munich, Vienna, New York, 1990, pp. 212–235.
15. B. Fisa, in *Composite Materials Technology,* P. K. Mallick and S. Newman, Eds., Hanser, Munich, Vienna, New York, 1990, pp. 303–317.
16. D. M. Bigg and J. R. Preston, *Polym. Compos.,* **10**(4), 261 (1989).
17. K. Friedrich and U. A. Karsch, *Polym. Compos.,* **3**(2), 65 (1982).
18. E. Jinen, *J. Mater. Sci.,* **22,** 1956 (1987).
19. M. G. Bader, in *Handbook of Composites,* A. Kelly and Yu N. Rabotnov, Eds., North-Holland, Amsterdam, New York, Oxford, 1983, Vol. 4, pp. 177–213.
20. V. K. Srivastava and S. Lal, *J. Mater. Sci.,* **26,** 6693 (1991).
21. J. F. Mandell, D. D. Huang, and F. J. McGarry, *Polym. Compos.,* **2**(3), 137 (1981).
22. K. Blizard and D. Baird, *Polym. Eng. Sci.,* **27,** 653 (1987).
23. K. C. Cole, D. Noel, and J. J. Heschler, *Polym. Compos.,* **9**(6), 395 (1988).
24. A. H. Kehayoglou, *Eur. Polym. J.,* **19,** 183 (1983).
25. G. Ives, J. Mead, and M. Riley, *Handbook of Plastics Test Methods,* Iliffe, London, 1971, p. 75, ASTM D792-66 Method B.
26. A. H. Kehayoglou and I. Arvanitoyannis, *Eur. Polym. J.,* **26,** 261 (1990).
27. J. M. Schultz, *Diffraction for Materials Scientists,* Prentice-Hall, Englewood Cliffs, NJ, 1982.
28. S. Kavesh and J. M. Schultz, *J. Polym. Sci. A-2,* **8,** 243 (1976).
29. C. K. Vonk, *J. Appl. Crystallogr.,* **6,** 148 (1973).
30. L. E. Alexander, *X-ray Diffraction Methods in Polymer Science,* Wiley-Interscience, New York, 1969.
31. W. Ruland, *Acta Crystallogr.,* **14,** 1180 (1961).
32. M. J. Richardson, in *Developments of Polymer Characterization-1,* J. V. Dawkins, Ed., Applied Science, London, 1978, pp. 205–244.
33. A. J. Waddon, M. J. Hill, A. Keller, and D. J. Blundell, *J. Mater. Sci.,* **22,** 1773 (1987).
34. J. K. DePorter, D. G. Baird, and G. L. Wilkes, *J. Macromol. Sci. Rev. Macromol. Chem. Phys.,* **33**(1), 1 (1993).
35. D. Bassett, R. Olley, and I. Al Raheil, *Polymer,* **29,** 1745 (1988).
36. W. Lee, B. Fukai, J. Seferis, and I. Chang, *Composites,* **19**(6), 473 (1988).
37. J. P. Bell and J. H. Dumbleton, *J. Polym. Sci. A-2,* **7,** 1033 (1969).
38. R. J. Watson and C. E. Chaffey, *Polym. Compos.,* **7,** 442 (1986).
39. G. Titomanlio, S. Piccaloro, and G. Marruci, *Polym. Eng. Sci.,* **25,** 91 (1985).
40. C. D. Han, *Multiphase Flow in Polymer Processing,* Academic Press, New York, 1981, Chap. 6.
41. S. Y. Hobbs, *Polym. Eng. Sci.,* **16,** 270 (1976).
42. A. F. Johnson, in *Encyclopedia of Materials Science and Engineering,* M. Bever, Ed., Pergamon Press, Oxford, New York, Toronto, 1986, Vol. 3, pp. 1979–2003.
43. V. K. Srivastava and P. S. Shembekar, *J. Mater. Sci.,* **25,** 3513 (1990).
44. W. Weibull, *J. Appl. Mech.,* **18,** 293 (1951).
45. M. F. Ashby and D. R. H. Jones, *Engineering Materials,* Pergamon Press, Oxford, New York, Toronto, Paris, 1985, pp. 59–61.
46. J. R. Lager and R. R. June, *J. Compos. Mater.,* **3,** 48 (1969).
47. F. W. Billmeyer, *Textbook of Polymer Science,* Wiley-Interscience, New York, 1984.
48. D. Blundell, R. Crick, B. Fife, J. Peacock, A. Keller, and A. Waddon, *J. Mater. Sci.,* **24,** 2057 (1989).

Received August 23, 1993
Accepted August 25, 1993